NASA TECHNICAL MEMORANDUM

NASA TM X- 64965

HIGH RESOLUTION FREQUENCY ANALYSIS TECHNIQUES WITH APPLICATION TO THE REDSHIFT EXPERIMENT

By R. Decher and D. Teuber

Space Sciences Laboratory
Science and Engineering

October 1975

NASA

George C. Marshall Space Flight Center
Marshall Space Flight Center, Alabama

TECHNICAL REPORT STANDARD TITLE PAGE

1. REPORT NO.	2. GOVERNMENT ACCESSION NO.	3. RECIPIENT'S CATALOG NO.
NASA TM X-64965		

4. TITLE AND SUBTITLE	5. REPORT DATE
High Resolution Frequency Analysis Techniques with Application to the Redshift Experiment	October 1975
	6. PERFORMING ORGANIZATION CODE
7. AUTHOR(S) R. Decher and D. Teuber	8. PERFORMING ORGANIZATION REPORT #
9. PERFORMING ORGANIZATION NAME AND ADDRESS George C. Marshall Space Flight Center Marshall Space Flight Center, Alabama 35812	10. WORK UNIT NO.
	11. CONTRACT OR GRANT NO.
	13. TYPE OF REPORT & PERIOD COVERED Technical Memorandum
12. SPONSORING AGENCY NAME AND ADDRESS National Aeronautics and Space Administration Washington, D. C. 20546	14. SPONSORING AGENCY CODE

15. SUPPLEMENTARY NOTES

Prepared by Space Sciences Laboratory, Science and Engineering

16. ABSTRACT

This report discusses high resolution frequency analysis methods with application to the Gravitational Probe Redshift Experiment (GP-A). For this experiment a resolution of 1×10^{-5} Hz is required to measure a slowly varying, low-frequency signal of approximately 1 Hz. Major building blocks include Fast Fourier Transform, Discrete Fourier Transform, Lagrange Interpolation, Golden Section Search, and Adaptive Matched Filter Technique. Accuracy, resolution, and computer effort of these methods are investigated, including test runs on an IBM 360/65 computer.

17. KEY WORDS	18. DISTRIBUTION STATEMENT
	Unclassified — Unlimited

19. SECURITY CLASSIF. (of this report)	20. SECURITY CLASSIF. (of this page)	21. NO. OF PAGES	22. PRICE
Unclassified	Unclassified	28	NTIS

For sale by National Technical Information Service, Springfield, Virginia 22151

TABLE OF CONTENTS

LIST OF ILLUSTRATIONS

ACKNOWLEDGMENTS

The authors gratefully acknowledge the assistance and cooperation of the Data Systems Laboratory and the Computer Sciences Corporation in the data analysis.

Mr. W. H. Walker from the Center Plans and Resources Control Office helped the data analysis by many stimulating discussions, his invaluable experience, and great interest.

HIGH RESOLUTION FREQUENCY ANALYSIS TECHNIQUES WITH APPLICATION TO THE REDSHIFT EXPERIMENT

I. INTRODUCTION

The data reduction of the Gravitational Probe Redshift Experiment (GP-A) requires the processing and analysis of low-frequency signals with a very high degree of accuracy and resolution. This report discusses various investigations of computation methods applicable to the data analysis of this experiment.

The objective of the GP-A is to test the equivalence principle by measuring the gravitational frequency shift of a hydrogen maser clock in a space probe. The frequency of the flight clock is compared with the frequency of an identical maser clock in the ground station while the space probe moves up and down through the gravitational field of the earth. The frequency comparison is accomplished by transmission of S-Band radio signals [1, 2]. Dr. Vessot of the Smithsonian Astrophysical Observatory (SAO) is the Principal Investigator. The experiment is scheduled for launch from Wallops Island in May 1976.

The "output signal" of the experiment is the beat frequency between the ground maser and the flight maser. This signal, which has a frequency of approximately 1 Hz, is recorded in digital form during the mission. The goal of the experiment is to test the equivalence principle to an accuracy of approximately $\pm 50 \times 10^{-6}$. To achieve this accuracy, the Redshift (gravitational frequency shift) contained in the beat signal must be determined with an accuracy of approximately $\pm 1 \times 10^{-5}$. (This figure includes a safety factor of 5 for errors in data processing.)

The frequency shift as a function of flight time predicted by theory is shown in Figure 1. The maximum fractional frequency shift is very small: $\Delta f/f \sim 5 \times 10^{-10}$. However, in terms of resolution required, one has to deal with a nonstationary process, and local frequency measurements are meaningless under these conditions.

The experiment data will be analyzed by comparing flight data with the theoretically predicted frequency shift derived from trajectory information obtained by tracking. According to theory, the Redshift has a linear dependence on the gravity potential difference $\Delta\phi$ (between the clock locations) expressed by $\Delta f/f = \alpha\Delta\phi/c^2$. The experiment will determine the value of $\alpha = 1 \pm \epsilon$ to an accuracy of $\pm\epsilon$ to test the linearity of this relationship (Fig. 2). Dr. Vessot has presented an overall data reduction scheme that is essentially based on signal processing in the time domain (processing of the phase of the beat frequency). This report investigates several methods of signal processing in the frequency domain which could be incorporated in the data reduction scheme or could be used as an alternate method to analyze data from the experiment. This alternate approach to data reduction would increase confidence in these results, in view of the extremely high requirements for experiment accuracy and the situation of a one-shot experiment.

Achieving the accuracy goal of the experiment requires not only careful analysis and design of flight hardware systems, but also of data reduction and computation methods. The computation methods [e.g., Fast Fourier Transform (FFT), Discrete Fourier Transform (DFT), and matched filter] discussed in this report are not new. However, applications of these methods with the resolution and accuracy requirements of the Redshift Experiment could not be found. The main objective was to investigate computation techniques with respect to the accuracy, resolution, and computer effort necessary for application to the Redshift Experiment data analysis. The IBM 360/65 computer was used for the test runs and simulated signal processing. The key to data reduction in the frequency domain is the adaptive filter technique implemented by the FFT. Samples of computer printouts have been included to show the small numbers and small changes involved in these computations.

II. GENERATION OF INPUT DATA

For the development and testing of computation methods, input data similar to the expected flight data had to be generated.

During the experiment, the beat frequency of the two masers (~ 1 Hz) will be processed by a 14-bit A/D converter with a sampling rate of 100/s and recorded in digital form on magnetic tape. To generate input data tapes, the frequency shift expected during flight (Fig. 1) was computed using the analytical expression:

$$\frac{\Delta f}{f} = \frac{GM}{c^2}\left(\frac{1}{r_1} - \frac{1}{r_2}\right) - \frac{1}{2c^2}\left(v_1^2 - v_2^2\right) + A \quad , \qquad (1)$$

where $GM/r_{1,2}$ is the gravity potential at the locations of the clocks, v_1 and v_2 are the velocities of the clocks in an inertial earth centered coordinate frame, c is the speed of light, and A includes acceleration terms. A predicted flight trajectory was used for the computations of the frequency shift according to equation (1). The first term in equation (1) represents the pure Redshift; the second term is the second order Doppler effect. (The first order Doppler effect is cancelled out by a special scheme of signal transmission and signal processing in the ground station.)

Three input data tapes covering three segments of the total flight time were prepared by Data Systems Laboratory using the UNIVAC 1108:

Input Data Tape 1 covers flight segment 500 to 3500 s.

Input Data Tape 2 covers flight segment 3500 to 6500 s.

Input Data Tape 3 covers flight segment 6500 to 9500 s.

The following information is contained on these tapes:

a. Flight time in seconds.

b. Gravitational frequency shift (pure Redshift) in Hertz.

c. Second order Doppler frequency shift in Hertz.

d. Additional frequency off-sets and variations to simulate hardware characteristics (for later implementation).

e. Combined frequency from 2, 3, and 4 in Hertz.

f. Aspect angle during flight.

Computations were made in double precision and transposed to tapes which are compatible with the IBM 360/65 computer on which all following evaluations were carried out. Each word on these tapes can be truncated in computations that correspond to the planned 14-bit A/D converter or to other bit numbers in the practical range of 8 to 16.

The sampling rate of the frequency is 100/s. There are 10 files per tape; each file contains 300 s of flight time. There are 10,000 time increments per 100 s interval corresponding to an array size of 10,000 in some of the following computations. A total useful experiment flight time of 9,000 s is equivalent to 900,000 time increments.

III. ANALYSIS BY PIECEWISE POLYNOMIAL FIT

For the frequency analysis of the Redshift Experiment, an averaging time interval of 100 s is considered optimum on the basis of the noise behavior and statistics of the hydrogen maser clock. As the clock moves up and down through the gravity field, the beat frequency changes continuously. This change is rather large compared to the resolution required (10^{-5}), as shown in Figure 3.

A piecewise polynomial curve fit to the frequency shift curve was tested as a first approach. This was done by taking the 10,000 data points in frequency and by calculating:

a. The least square polynomial fit by orthogonal polynomials

b. The polynomial coefficients

c. The fitted values for each time point (100 s interval)

d. The residuals between actual and fitted segments

e. The mean and the standard deviation of residuals.

Figures 4 and 5 show typical computer printouts for two different segments of flight time for the coefficients of the polynomial giving a beat frequency:

$$f = a_0 + a_1 t + a_2 t^2 + a_3 t^3 + a_4 t^4 + a_5 t^5 \ .$$

Also, the mean and standard deviation for increasing order of polynomial fit are given in Figures 4 and 5. Central Processor Unit (CPU) time for all fits is approximately 15 minutes.

The result shows that the mean of the residuals decreases with increasing order of polynomial fit (as one would expect), but the spread of the residuals increases. It is therefore not possible to match the frequency curve by a polynomial fit with the required accuracy. The polynomial approach is not converging because of the dynamic behavior of the frequency change which is described by the relatively complicated analytical function for the frequency shift [equation (1)].

IV. SPECTRAL RESOLUTION AND UNCERTAINTY PRINCIPLE

The uncertainty relation [3] states that the equivalent widths of a function and its transform are reciprocals:

Equivalent duration × equivalent bandwidth = 1 .

This implies that if a stationary Redshift signal of 1 Hz had to be observed in real time to a resolution of one part in 100,000, the experiment time would have to be 10^5 or 27.7 h. In the digital data analysis, a required spectral resolution exceeding the limits imposed by the observation time can be obtained by artificially extending the original data sequence with zeros.

To test this technique, a finite sinusoidal pulse corresponding to a frequency of 1 Hz was analyzed with the FFT and DFT. The required computational steps are shown by the flow diagram of Figure 6. The sharpening of the spectral line, i.e., the increased resolution of the finite length pulse extended by adding zeros, depends on the following parameters according to the relationship between the time and frequency domains:

N — The number of samples taken to represent the time function; this is the data block size, normally to base 2 in the FFT [4,5].

Δt — The sample interval, i.e., the time between samples.

T — Total length of record $T = N\Delta t$.

N/2 — The number of frequency points in the spectral representation; this is half the data block size because the frequency information is broken into two displays of real (magnitude) and imaginary (phase) part.

Δf — Frequency resolution or the number of Hertz between frequency points (spectral lines).

F_{max} — The maximum frequency of the spectral display.

Time and frequency domains are related by Sharnon's theorem,

$$\Delta t = \frac{1}{2 F_{max}} \quad ,$$

and the frequency resolution is given by the total length T of the recorded time function,

$$\Delta f = \frac{1}{T} \quad .$$

Therefore, changing one of these parameters will change the other quantities.

The signal to be analyzed for the Redshift Experiment is sampled at a rate of 100/s by the A/D converter, which means $\Delta t = 0.01$ s. In this case, the frequency resolution Δf of the spectral analysis for different data block sizes N is as follows:

$N = 2^{16} = 65,536$ $\Delta f = 0.0015$ Hz

$N = 2^{21} = 2,097,152$ $\Delta f = 0.000048$ Hz

$N = 2^{23} = 8,388,608$ $\Delta f = 0.000012$ Hz

A computer printout of the spectral analysis representation for the case $N = 2^{16}$ and $f = 1$ Hz is shown in Figure 7. Figure 7 represents only a small portion of the printout which contains 32,768 spectral elements. The frequency points (spectral lines) are given by the letter R displaying the sin x/x shape in discrete form. The separation between two adjacent spectral lines corresponds to 0.0015 Hz. The maximum amplitude (4930) occurs at the 328th spectral element. The computations were performed with an IBM 360. The maximum length of the array size of 2^{16} that can be stored in the computer will set a limit to the total length of record (i.e., frequency resolution) in-core

computation. With additional disk memory, much larger arrays can be transformed at the expense of computing time and obtaining superfluous information. However, in high resolution spectral analysis, computation time and effort can be reduced by computing spectr l elements over a selected limited range of the spectrum [6]. A flow diagram of this process is shown in Figure 8. A computer routine scans the output vector of the FFT to find the spectral element of maximum magnitude. A three-point Lagrange interpolation within three spectral elements is then applied and a new block size N is selected to compute fewer spectral elements with higher resolution using the DFT [5].

Typical results of such a selective computation are represented in Figure 9 showing the occurrence of the maximum magnitude of the spectral elements. A block size of $N = 2^{16}$ was selected for the FFT (corresponding to a 100 s beat frequency interval). The DFT for 50 spectral lines with $N = 2^{23}$ was used to obtain the high resolution of $\Delta f = 0.000012$ Hz. The fastest and most versatile version of the FFT was used on the IBM 360 computer [7]. Typical runs on the machine are characterized by in-core mode with 650 K-byte memory required. CPU time was approximately 2 min, including 7 s for the 65 K FFT.

The technique was applied to certain segments of the simulated Redshift signal tapes. The results for two segments with different frequency change rates are shown in Figure 10. The 500 to 600 s interval is at the beginning of the trajectory and the 3500 to 3600 interval is near apogee.

The conclusion obtained from these tests is that the FFT and DFT combined will resolve a stationary signal or pulse train to some parts in 100,000 when the record length is extended with a sufficient number of zeros. The methods could be of value to analyze quasi-stationary signals such as those caused by the spinning motion and dynamics of the spacecraft. In these cases, however, the utmost resolution would not be required. During a short interval at apogee, the frequency change will be slow enough to use the FFT and DFT methods to determine the beat frequency with high resolution. Except for this short period, the Redshift signal cannot be extracted directly by spectral analysis because the nonlinear frequency change with time prohibits an interpretation of the spectrum. Consequently, a matched filter technique described in the succeeding section was pursued as the next approach for analysis of the beat signal.

V. MATCHED FILTER TECHNIQUE

In many signal processing applications, the use of the matched filter technique yields optimum results. This technique has been widely used for processing radar signals [8,9]. A matched filter has a frequency response that is the complex conjugate of the spectrum of the input signal. The output of the normal matched filter closely approximates the sin x/x form, which has high side lobes, the largest of which is some 14.5 dB below the main lobe. Such side lobes can be reduced by application of a spectrum weighing function. A cosine bell was chosen to provide time domain Hanning. Tapering is performed in a circular manner so that an even function will remain even and side lobes are reduced to approximately 40 dB.

Figure 11 shows a flow chart for a linear frequency modulated matched filter test case. The magnitude of the frequency sweep is comparable to the frequency change of the Redshift beat signal. Analytically generated FM signals were used to check the program.

The signal $A(I,1) = \cos(\omega t + \beta t^2)$ is compared in a matched filter with signals of the form $B(I,1) = \cos \omega t + \alpha_K \beta t^2)$, with the templates

$$\alpha_1 = 0.99995$$

$$\alpha_2 = 1.00000$$

$$\alpha_3 = 1.00005 \ .$$

The dc output (zero element) of the matched filter indicates the best fit for $\alpha_2 = 1.00000$, which corresponds to a match of the signal to itself. The mathematics of the single-tone frequency modulation can be found in Reference 10.

An example of computer printout data showing the first 100 elements of the matched filter output for the three different α_K is given in Figure 12. The result verifies the correct programming and soundness of approach. The CPU time for a block size of 32,768 elements and including seven FFT operations was approximately 2 min. Even though it takes the whole memory of the IBM 360/65 computer with 650 K bytes, the time required for the analysis of the complete Redshift flight data would be only several hours CPU time. In the case of 65 consecutive evaluations of 100 s segments along the trajectory, total CPU time would be approximately 7 h.

VI. ADAPTIVE MATCHED FILTER ANALYSIS

The process of matching two signals with varying frequencies optimally in data processing is best automated via the Golden Section Search. In the case of the Redshift Experiment, one signal would be the beat frequency measured during flight and the second signal would be the computed beat frequency obtained from tracking data and theory [11].

The Golden Section Search which is an iterative process to find the maximum (or minimum) of unimodal functions is based on the iteration by Fibonacci numbers which are defined by:

$$Y_{n+1} = Y_n + Y_{n-1} \quad \text{with} \quad Y_0 = 0 \quad \text{and} \quad Y_1 = 1 \quad .$$

For example,

$Y_0 = 0$ $\quad$ $Y_4 = 3$ $\quad$ $Y_8 = 21$

$Y_1 = 1$ $\quad$ $Y_5 = 5$ $\quad$ $Y_9 = 34$

$Y_2 = 1$ $\quad$ $Y_6 = 8$ $\quad$ $Y_{10} = 55$

$Y_3 = 2$ $\quad$ $Y_7 = 13$ $\quad$ $Y_{11} = 89$

The sequence of Y numbers represents the strategy for selecting subdivisions along the X axis in the range where the maximum of a function is expected. Figure 13 shows that the Golden Section Search converges fast to a fraction of the original interval of uncertainty. For comparison, a progressive step search and a search by interval halving are also shown in Figure 13. [The ratio between two consecutive numbers of the Golden Section Search approaches the golden ratio: $(1 + \sqrt{5})/2$.]

An adaptive matched filter process using the Golden Section Search was implemented on the IBM 360/65 computer. The corresponding flow chart is shown in Figure 14. The input tapes (described in Section II) provided the simulated beat frequency (Redshift signal). For the purpose of this exercise,

the input signal is split to provide the two signals to be matched. The Golden Section Search method changes one of the signals for each run through the matched filter and determines the quality of the template fit. The fit is expressed by $\alpha = (1 \pm \epsilon)$, with ϵ representing the deviation. Starting with an initial offset of $\epsilon = \pm 0.00005$, the best fit was obtained for $\alpha = 1.000000$ (or $\epsilon = 0.000000$) with very few iterations as expected. ($\alpha = 1.000000$ represents a match of a signal to itself.) Ten min of CPU time was required for a 100 s data interval containing 10,000 points. The FFT requires 650 K byte memory and 32,768 element block size. The computer runs performed verified the software design. In addition, the following tests were performed:

a. Noise from a random number generator was superimposed on both the amplitude and phase of the beat signal. The results showed, as expected, that the matched filter provides optimal noise rejection [8,9].

b. To demonstrate that the 14-bit A/D converter will be sufficient for the ground station, the computed amplitude of the beat frequency signal was truncated corresponding to 10, 12, 14, and 16 bits. The matched filter output remained maximal at dc for $\alpha = 1.000000$.

c. It is possible to extend the search method to more than one parameter, e.g., for additional functions of frequency or phase shift. However, one quickly arrives at insurmountable difficulties for more than two parameters, since both local and global optima are entering the picture. Search for additional parameters amounts to cross-correlation techniques that are best done in the frequency domain [5]. For this reason, the method of extending records with zeros was maintained.

VII. APPLICATION TO REDSHIFT DATA REDUCTION

Figure 15 outlines one of several possible schemes for application of the adaptive matched filter technique to the reduction of Redshift flight data. The scheme has not been implemented yet. One of the inputs required for a simulation run consists of the hardware calibration functions that will be generated during the test program of the payload. A brief discussion of the content of building blocks in Figure 15 is presented as follows:

Block 1 is the digitized beat frequency (i.e., amplitude samples) measured during the experiment and recorded on magnetic tape.

Block 2 represents the FFT applied to the signal from Block 1 before input to the matched filter. The DFT and regression analysis (2A and 2B) of the flight data provide information concerning frequency shifts and modulation effects related to payload spin and spin axis motion if present in the original signal [12].

Block 3, the matched filter, correlates the measured frequency shift with the computed expected frequency shift generated by several other blocks discussed hereinafter.

Block 4, the output of the matched filter, generates the error signal ϵ to control the Golden Section Search for an optimum match of the two signals via Blocks 5 and 6. The ϵ that is applied to the pure Redshift signal only is iterated until the best fit is achieved. The remaining ϵ value is a measure of agreement between theoretical and measured Redshift.

Block 7 combines the frequency from several sources to generate the expected/corrected signal input for the matched filter.

Block 8 changes frequency to amplitude, and Block 9 applies the FFT.

Block 10 provides the flight trajectory data for computation of the Redshift in Block 11 and computation of the second order Doppler effect in Block 12.

Block 13 generates frequency correction to be applied to the computed frequency shifts in Block 7. These frequency corrections are obtained from hardware calibrations, telemetry data indicating the actual flight conditions, and trajectory information. Corrections which can be applied include magnetic field effects, centrifugal force on the maser cavity, zero-g effect on the maser cavity, antenna characteristics, ambient pressure change, and others. The resolution of the computational process itself is several orders of magnitude above the level set as the goal for the experiment ($\epsilon = \pm 0.00001$), as has been tested and demonstrated in previous sections.

VIII. CONCLUSIONS

The frequency shift experienced by the flight maser is a nonstationary event during the entire spacecraft flight within the required spectral resolution of 50 parts in a million. A regression analysis of computed frequencies shows that the frequency changes are nonlinear within the sample interval of 100 flight s and that any least square polynomial fit through the computed Redshift will deviate incompatibly within the required resolution.

A similar result was obtained by a spectral analysis using the FFT at medium resolution (0.001) and a DFT at high resolution (0.00001). Again, the determination of an instantaneous frequency at the required resolution is incompatible with the nonstationary Redshift event.

Matching a measured ensemble to a predicted ensemble in the frequency domain by a matched filter will provide the means to evaluate the experiment data to the required accuracy. The two obvious constraints to this are: (1) the expected frequency shift obtained from spacecraft tracking and hardware calibrations have to be known to an accuracy better than the desired experiment accuracy, and (2) the signal that represents the beat frequency between ground and flight maser (after first order Doppler elimination) must not be degraded by the data recording more than dictated by the desired experiment accuracy.

An adaptive search for the best fit between the computed and measured signal will determine to what accuracy the equivalence principle has been verified by the flight experiment in the evaluation of ϵ, a measure of the similarity between expected and measured results.

The matched filter in general provides four desirable advantages for the data reduction:

a. The evaluation is in the frequency domain. The transform necessary for this is an averaging process that forms essentially sums of products and utilizes more information than, for example, Events Per Unit of Time (EPUT) methods [13].

b. The matched filter has optimal noise rejection. The noise level in the simulated maser beat signal was set in test runs to several orders above the expected signal, and the same results were obtained as with zero noise.

c. The matched filter output is invariant to a constant phase shift between expected and actual signal. A phase shift that is known to be proportional to time is detected by the output of the matched filter and can be corrected.

d. The FFT at the matched filter input will aid the overall signal identification and separation as a "quick-look" means to detect payload spin decay, wobble, or other unexpected malfunctions.

The computing times in the IBM 360/65 computer proved to be modest and practical. It takes approximately 7 min CPU time to determine the best fit between a simulated ground signal and an expected Redshift signal for any 100 s flight interval to $\epsilon \leqq 0.00005$.

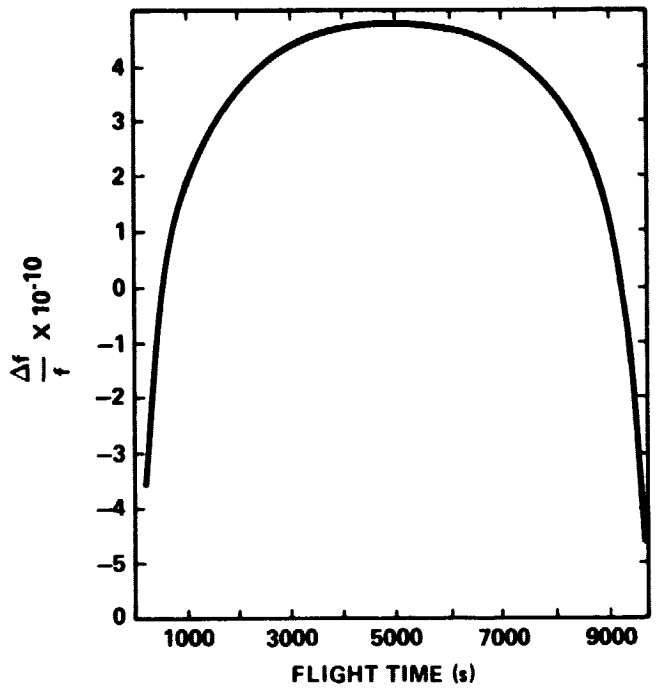

Figure 1. Fractional frequency shift versus flight time.

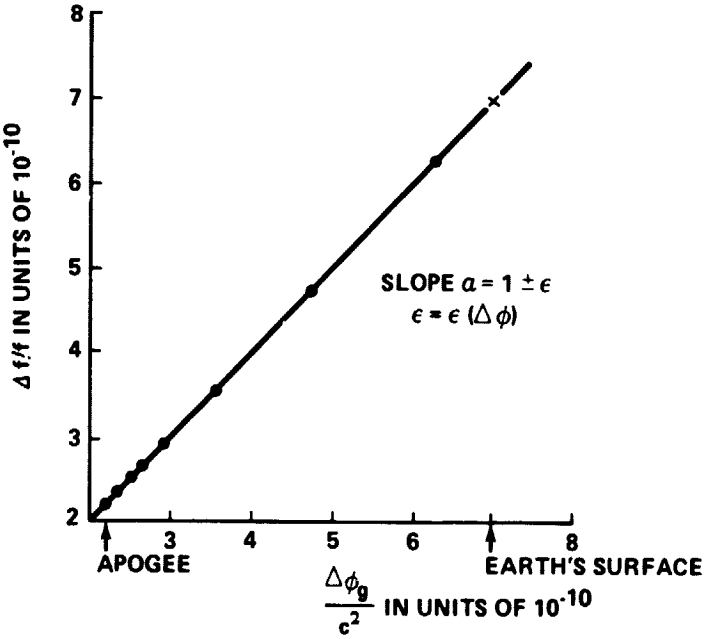

Figure 2. Comparison of theory and flight data.

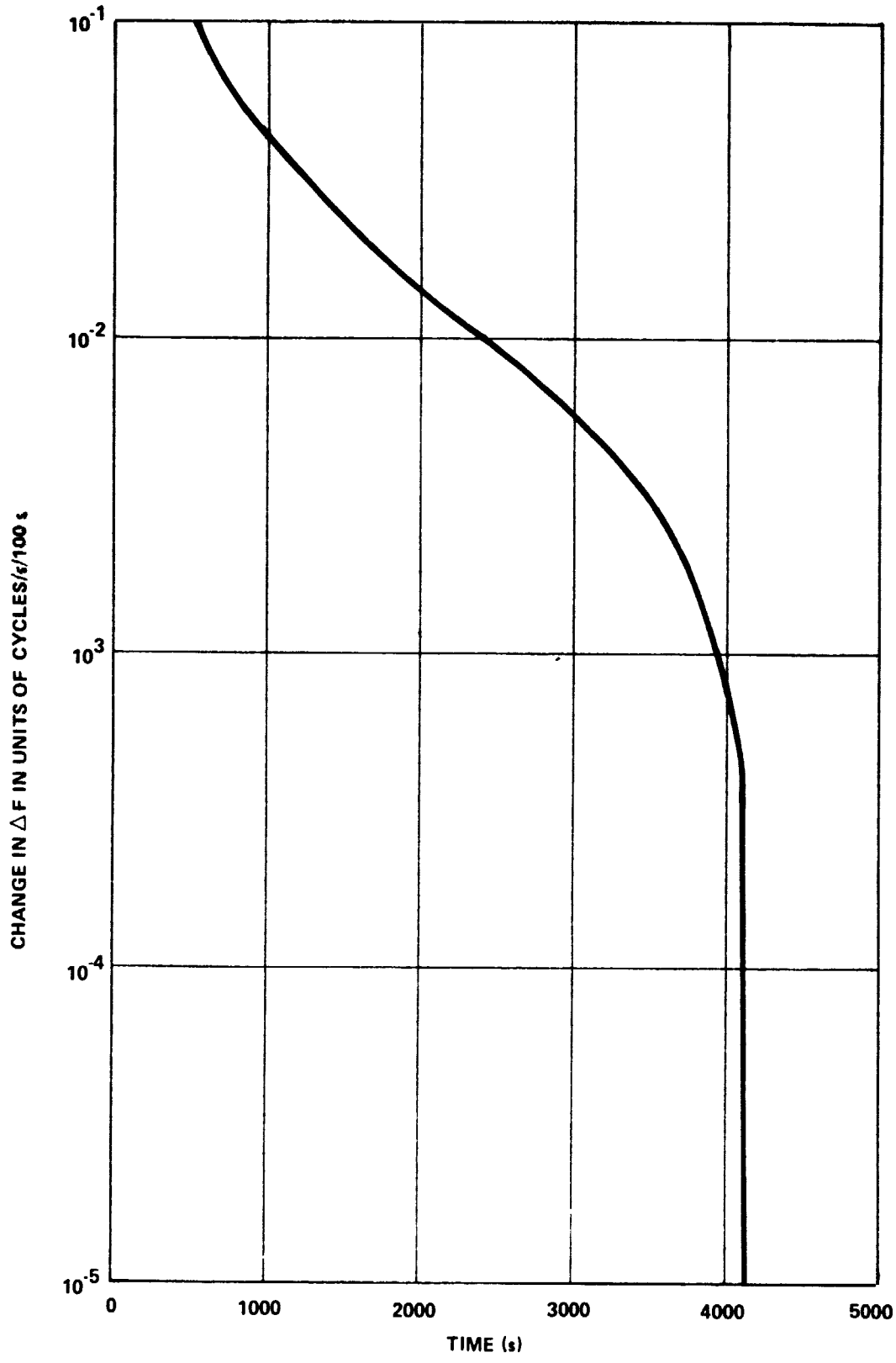

Figure 3. Rate of frequency change.

```
TIME =     600.00   FREQ =   0.33869658E-01
TIME =     601.00   FREQ =   0.34673687E-01
TIME =     602.00   FREQ =   0.35476193E-01
TIME =     603.00   FREQ =   0.36277194E-01
TIME =     604.00   FREQ =   0.37076678E-01
TIME =     605.00   FREQ =   0.37874650E-01
TIME =     606.00   FREQ =   0.38671125E-01
TIME =     607.00   FREQ =   0.39466087E-01

(FIT THRU 10,000 POINTS)

TIME =     690.00   FREQ =   0.10041571E 00
TIME =     691.00   FREQ =   0.10109878E 00
TIME =     692.00   FREQ =   0.10178077E 00
TIME =     693.00   FREQ =   0.10246152E 00
TIME =     694.00   FREQ =   0.10314113E 00
TIME =     695.00   FREQ =   0.10381955E 00
TIME =     696.00   FREQ =   0.10449678E 00
TIME =     697.00   FREQ =   0.10517287E 00
TIME =     698.00   FREQ =   0.10584784E 00
TIME =     699.00   FREQ =   0.10652161E 00
```

2	0.3382838E-01	0.7595664E-03	-0.6119424E-06		
	0.5228436E-04	0.1092145E-03			
3	0.3406728E-01	0.7672335E-03	0.1051678E-06	-0.4782457E-08	
	0.5212403E-04	0.1065868E-03			
4	0.3410648E-01	0.7685064E-03	0.4079536E-06	-0.9490190E-08	0.2353243E-10
	0.5214244E-04	0.1670030E-03			
5	0.3355332E-01	0.9247046E-03	-0.1108924E-04	0.2972492E-06	-0.3428844E-08	0.1381471E-10
	0.5172686E-04	0.2470165E-03			

Figure 4. Typical computer printout for least square polynomial frequency fit, 600 to 700 seconds flight time.

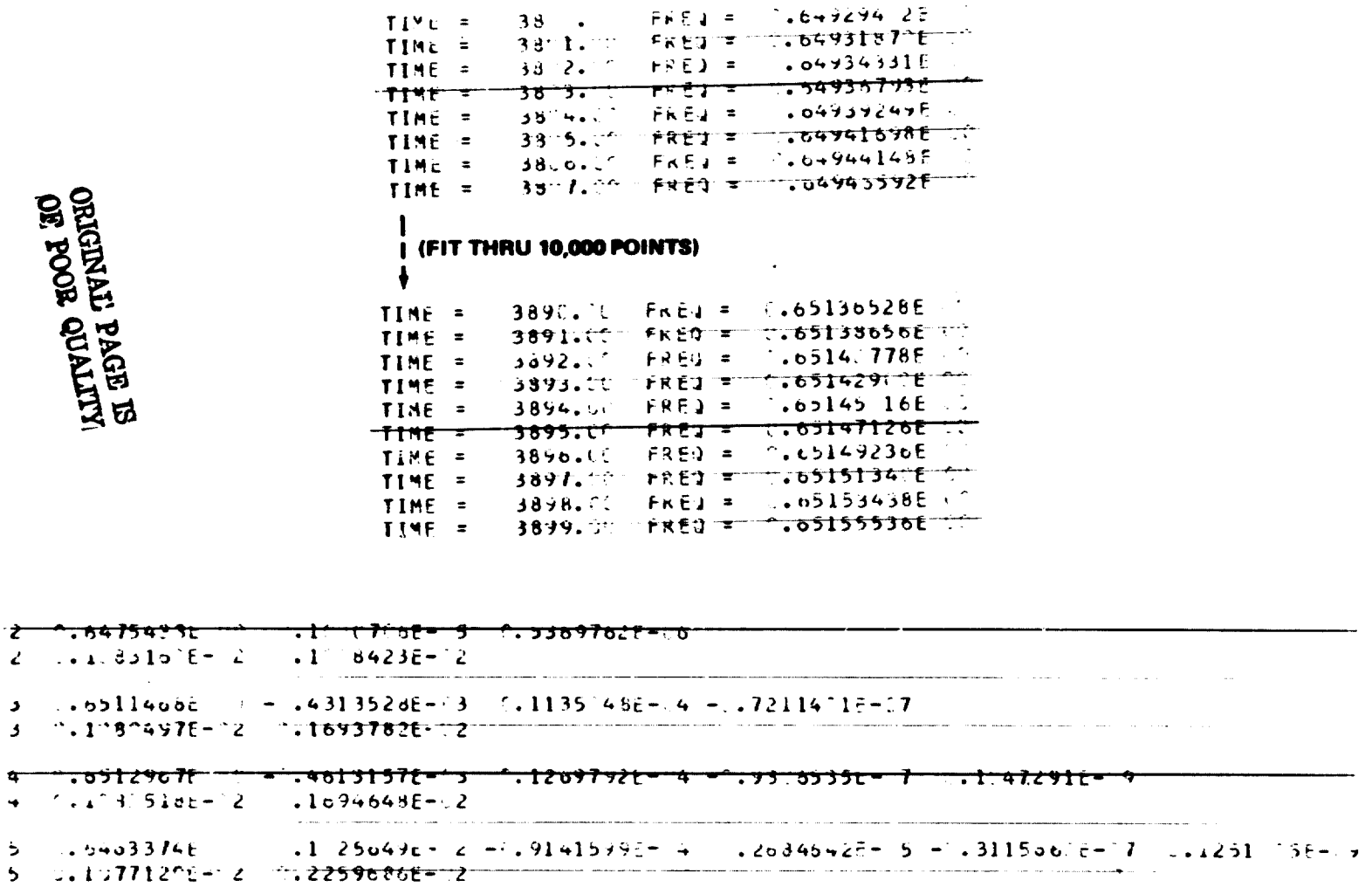

Figure 5. Typical computer printout for least square polynomial frequency fit, 3800 to 3900 seconds flight time (near apogee).

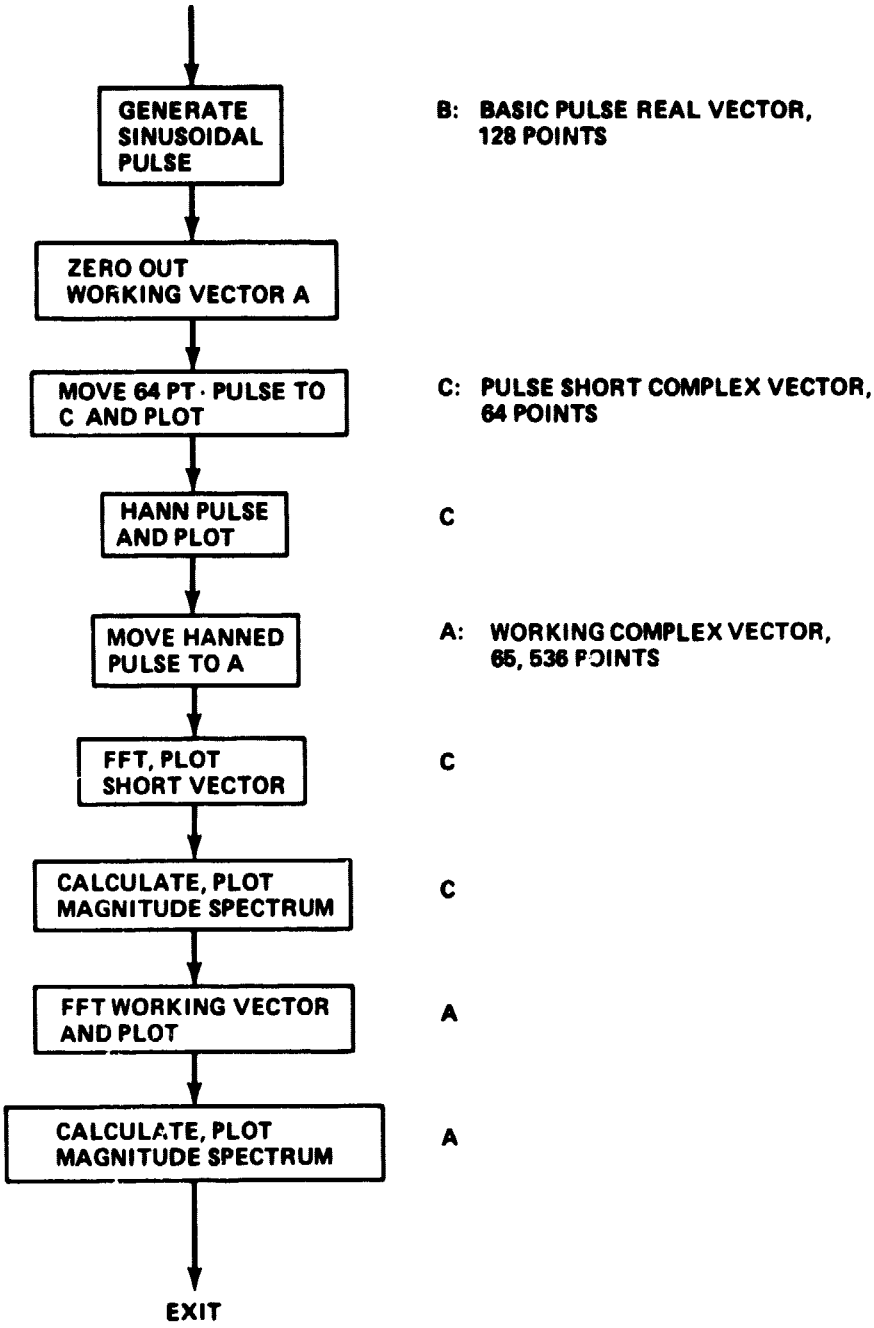

Figure 6. Uncertainty principle test using finite sinusoidal pulse, FFT.

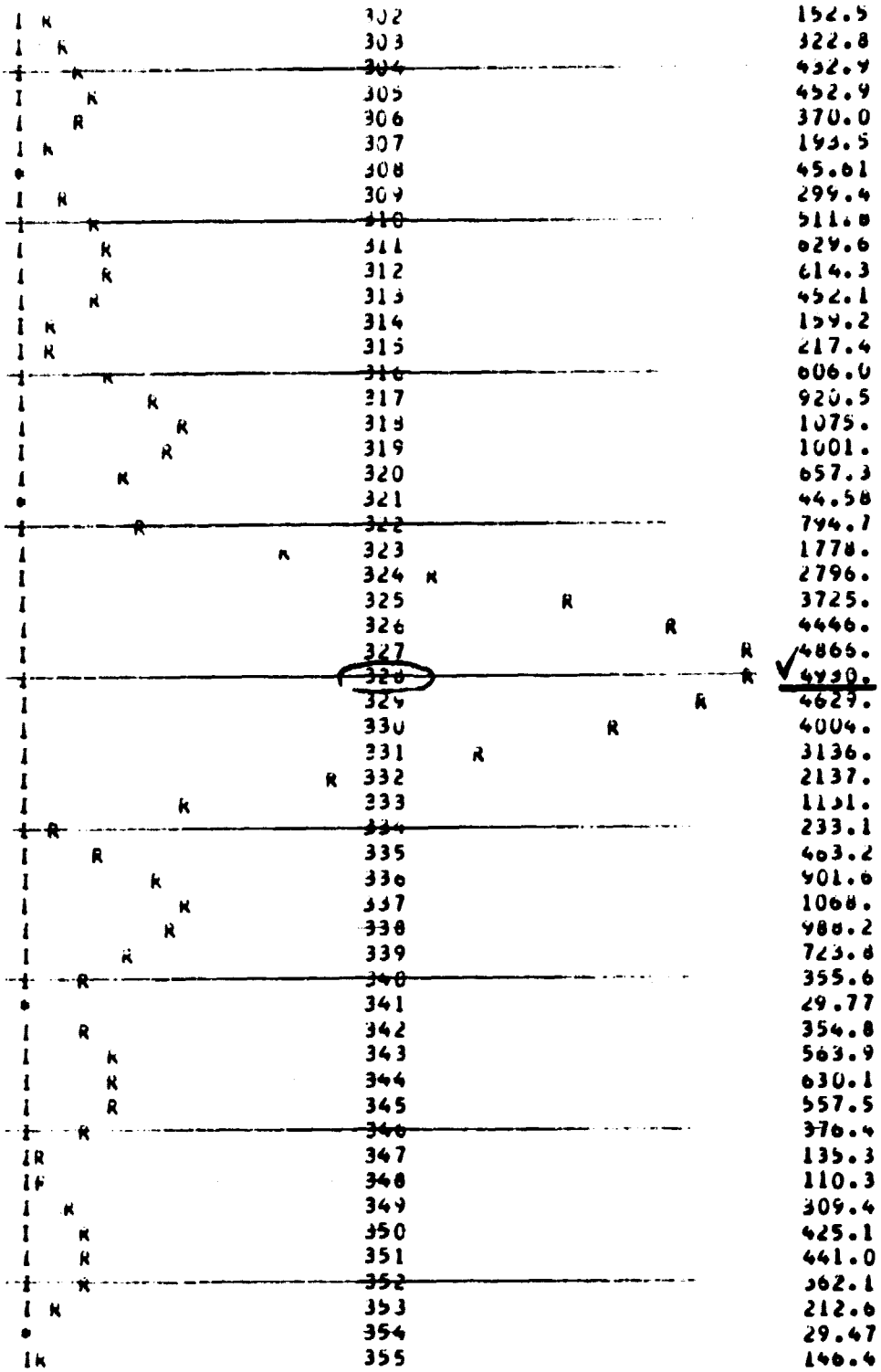

Figure 7. FFT spectral analysis of finite sinusoidal pulse (1.0 Hz).

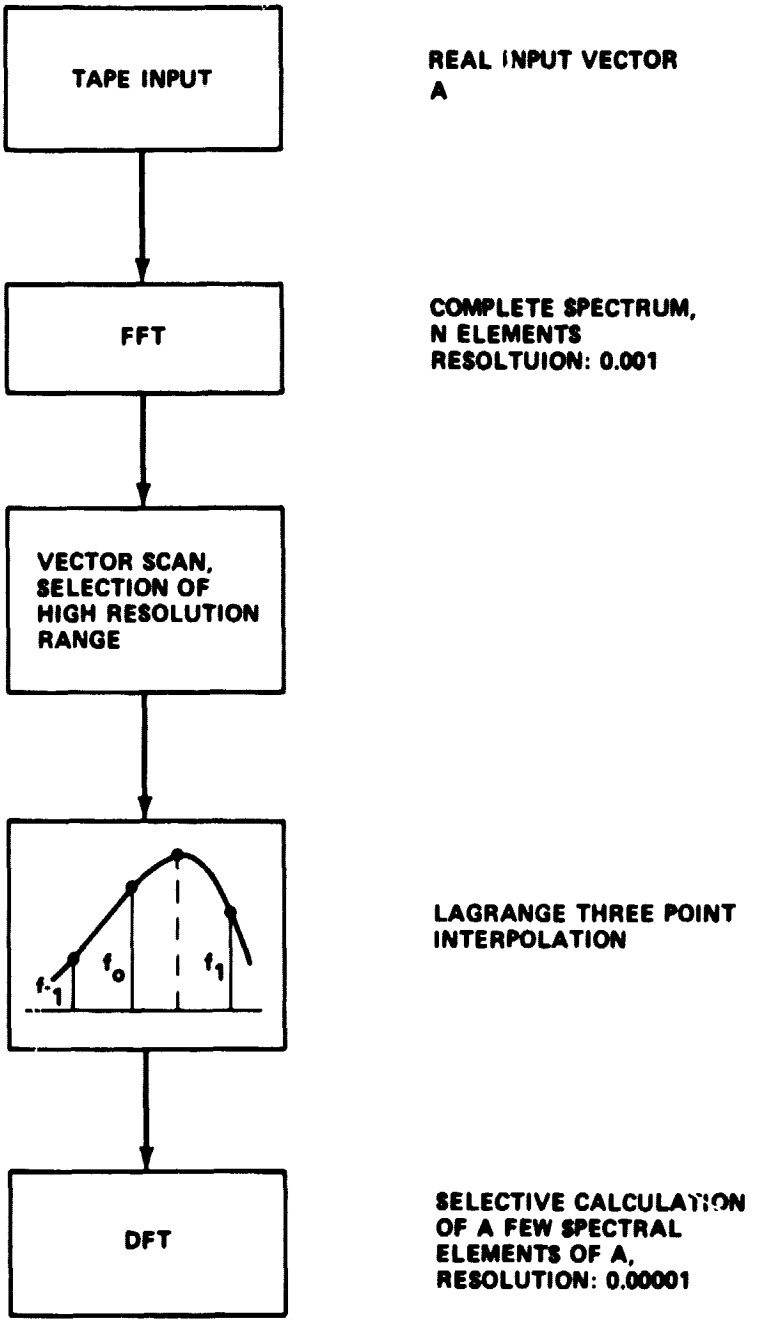

Figure 8. FFT, Lagrange interpolation, and DFT for high spectral resolution.

```
 0.48896016E 04  0.49066750E 04  0.49227031E 04  0.49377C81E C4  0.49459922E 04  0.49614
0.49869141E 04  0.49924336E 04  0.49964648E 04  0.49990000E 04  0.50000391E 04  0.499958
                                                                        13

0.49892422E C4  0.49820886E 04  0.49748900E 04  0.49654844E 04  0.49546C55E 04  0.494225
0.48904141E 04  0.48782385E 04  0.48586209E 04  0.48376010E 04  0.48151602E 04  0.479132
0.47711535E 04  0.47462305E 04  0.47215977E 04  0.46979043E 04  0.46806403E 04  0.465180
0.46408438E 04  0.46013984E C4  0.45607734E 04  0.45189922E 04  0.4276C7C3E 04  0.423203
0.41934012E C4
```

FIRST SPECTRAL ELEMENT TO BE CALCULATED (ZERO ORIGIN) LS = 5230

NUMBER OF SPECTRAL ELEMENTS TO BE CALCULATED LN = 50

Figure 9. Part of DFT printout.

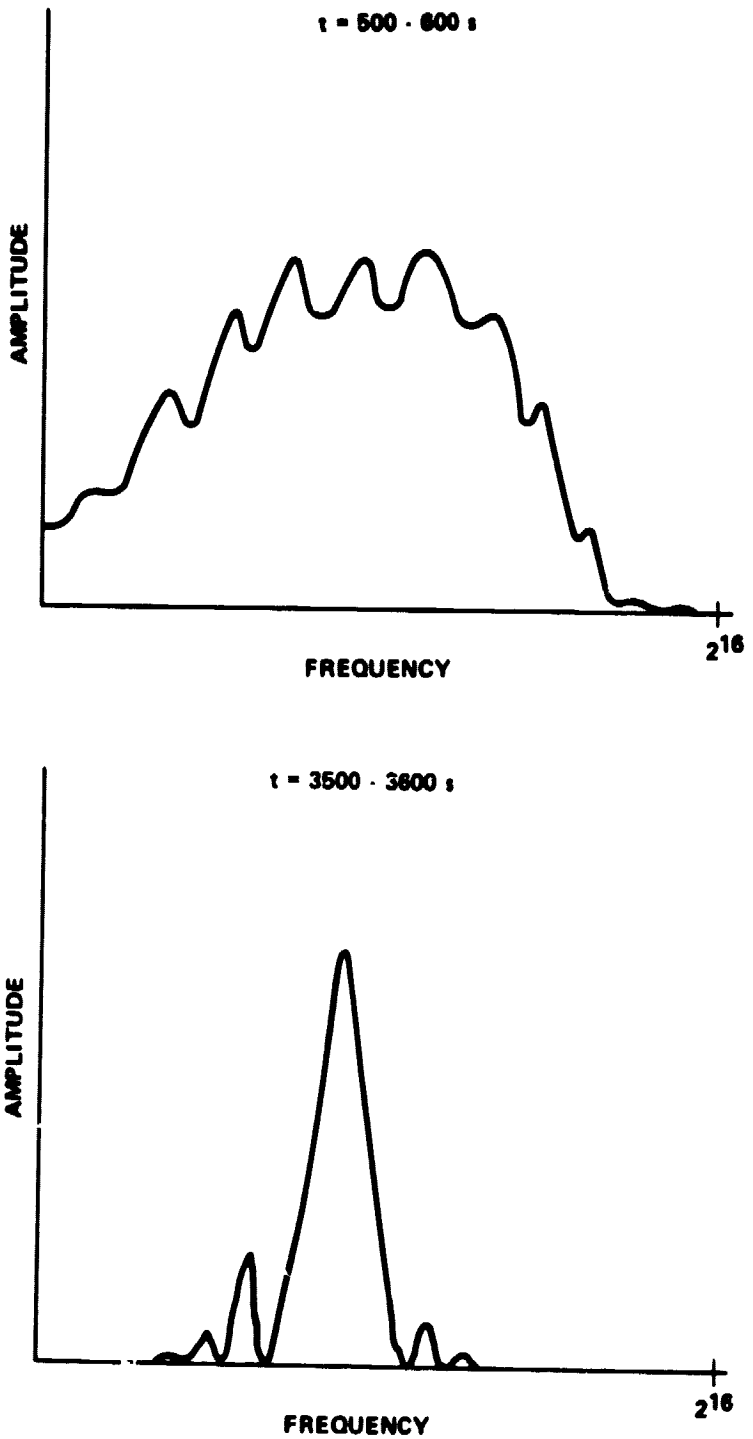

Figure 10. Typical spectra of simulated beat signals.

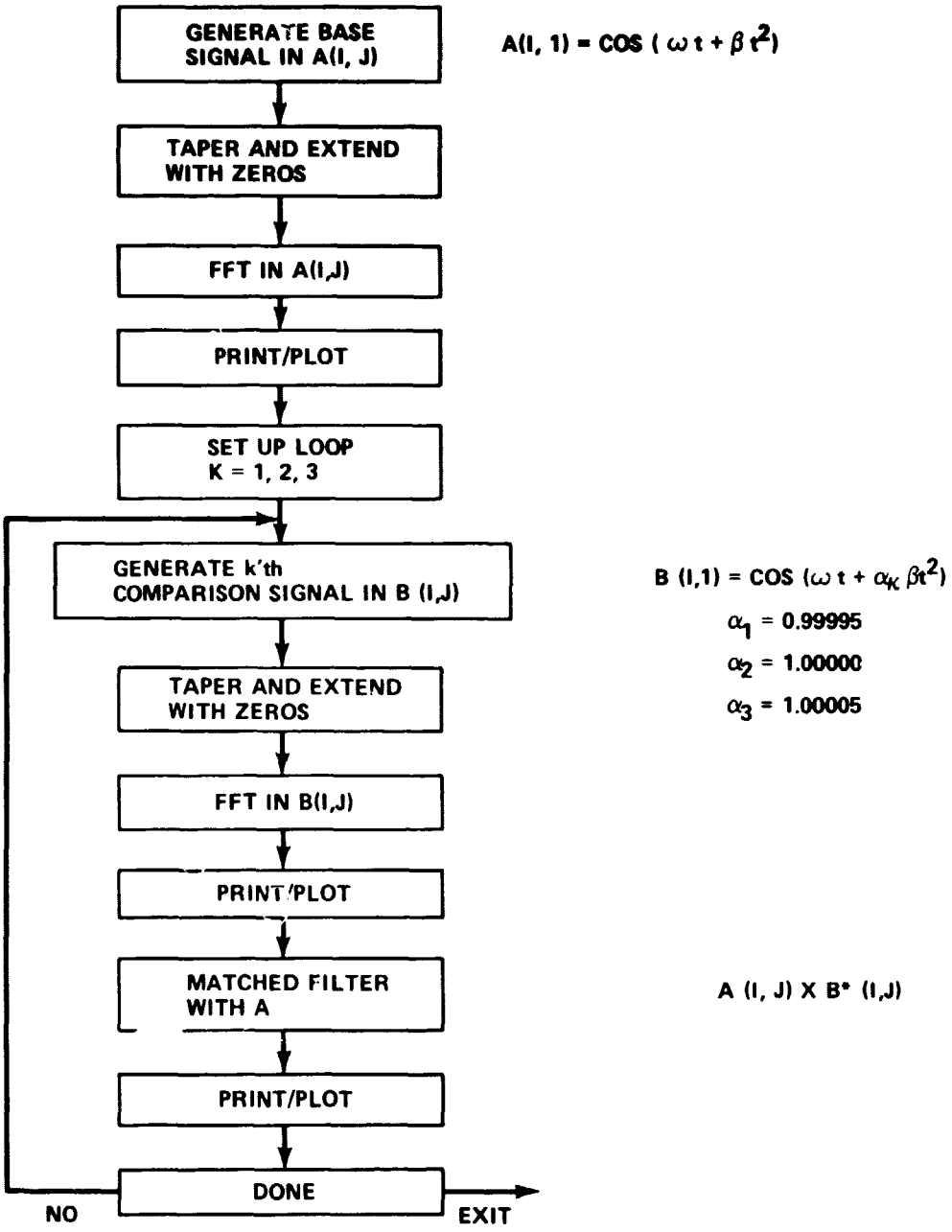

Figure 11. Matched filter method flow chart.

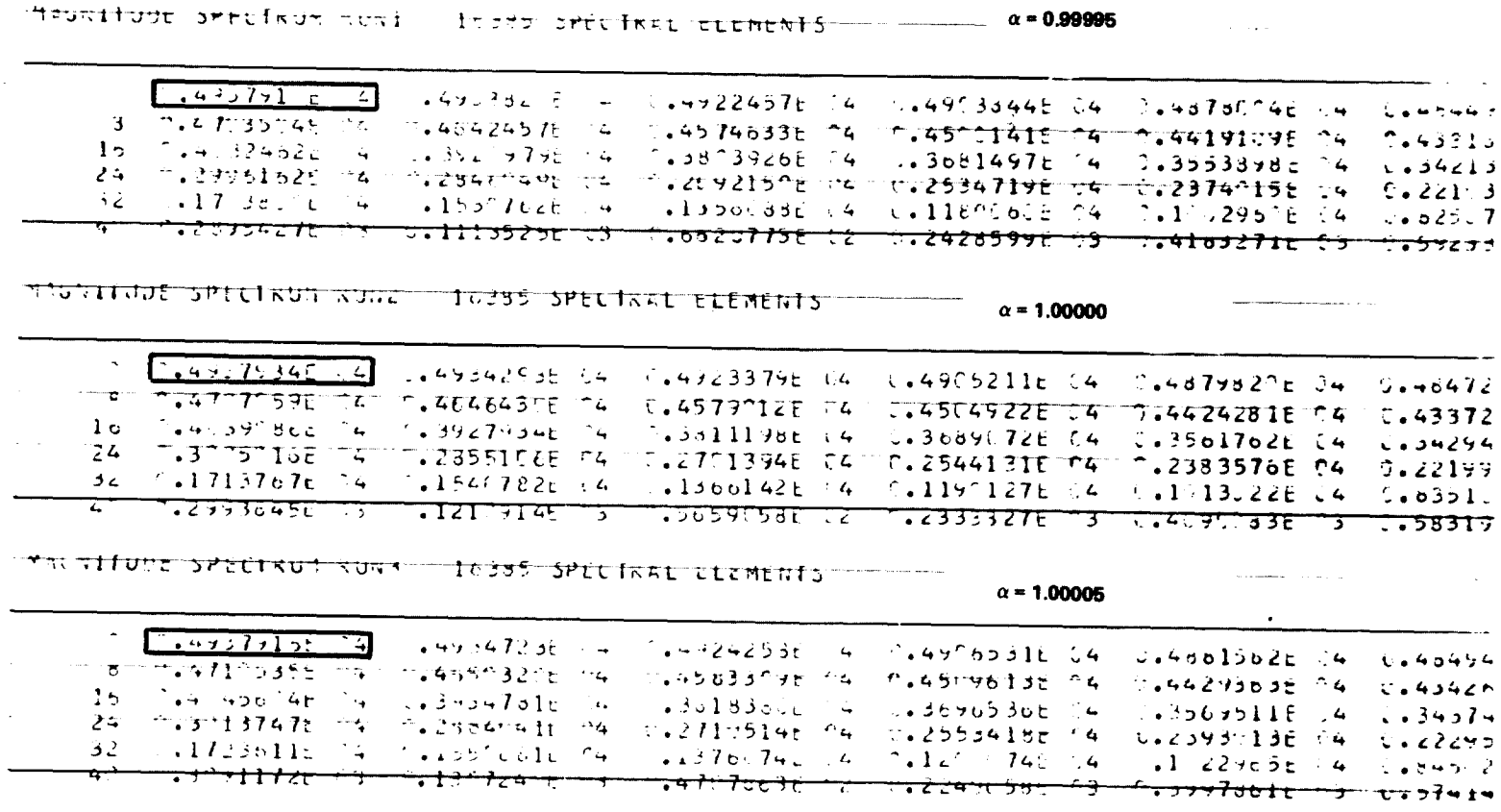

Figure 12. Matched filter data printout.

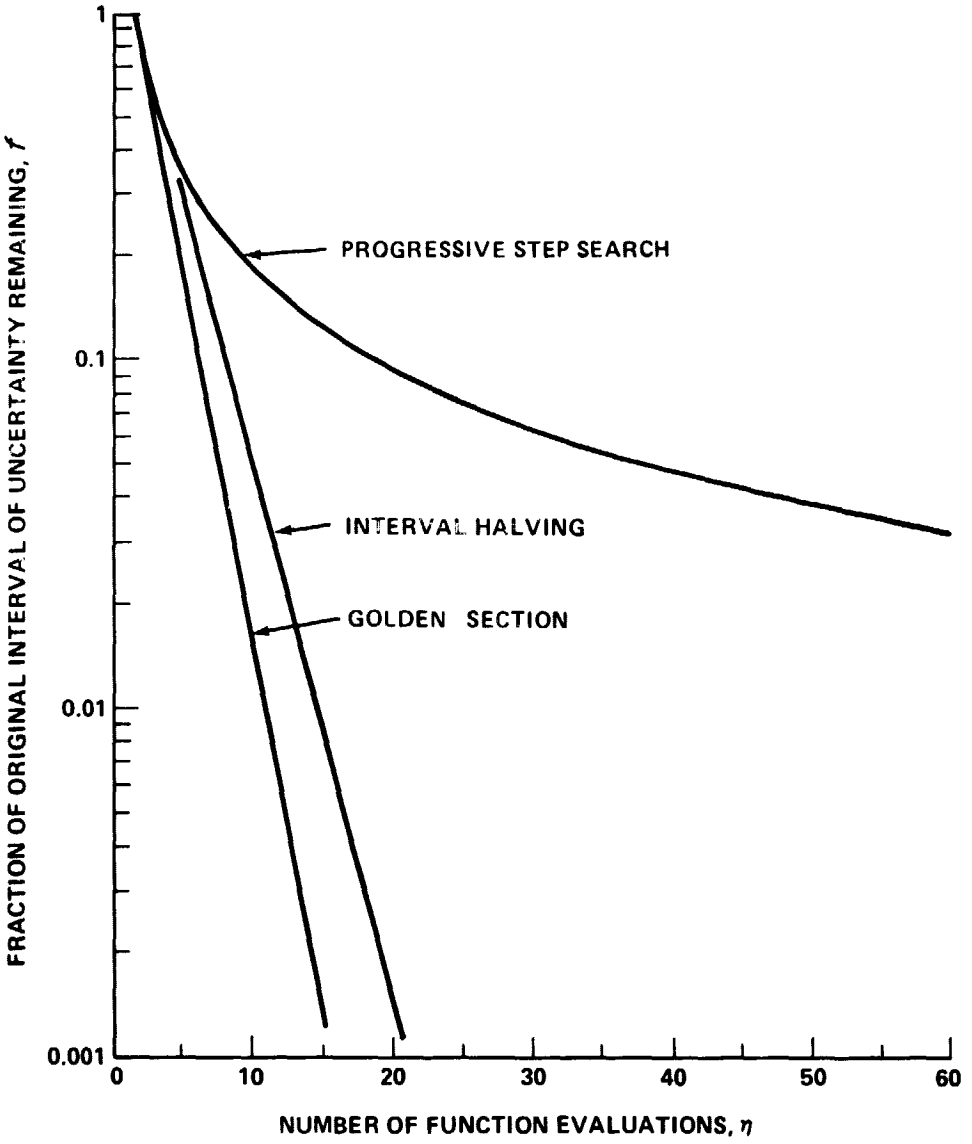

Figure 13. Convergence of different search methods.

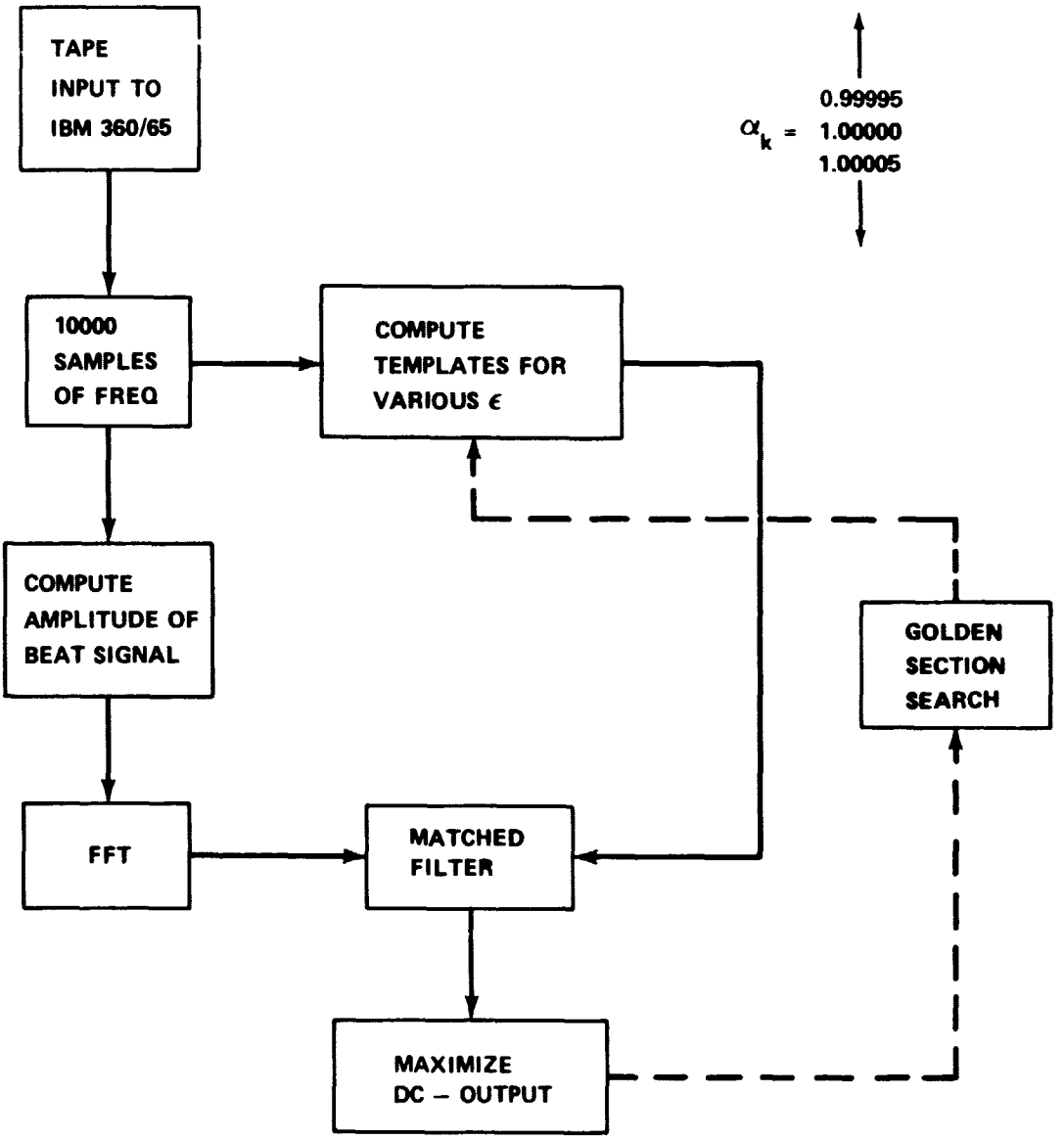

Figure 14. Adaptive matched filter flow chart.

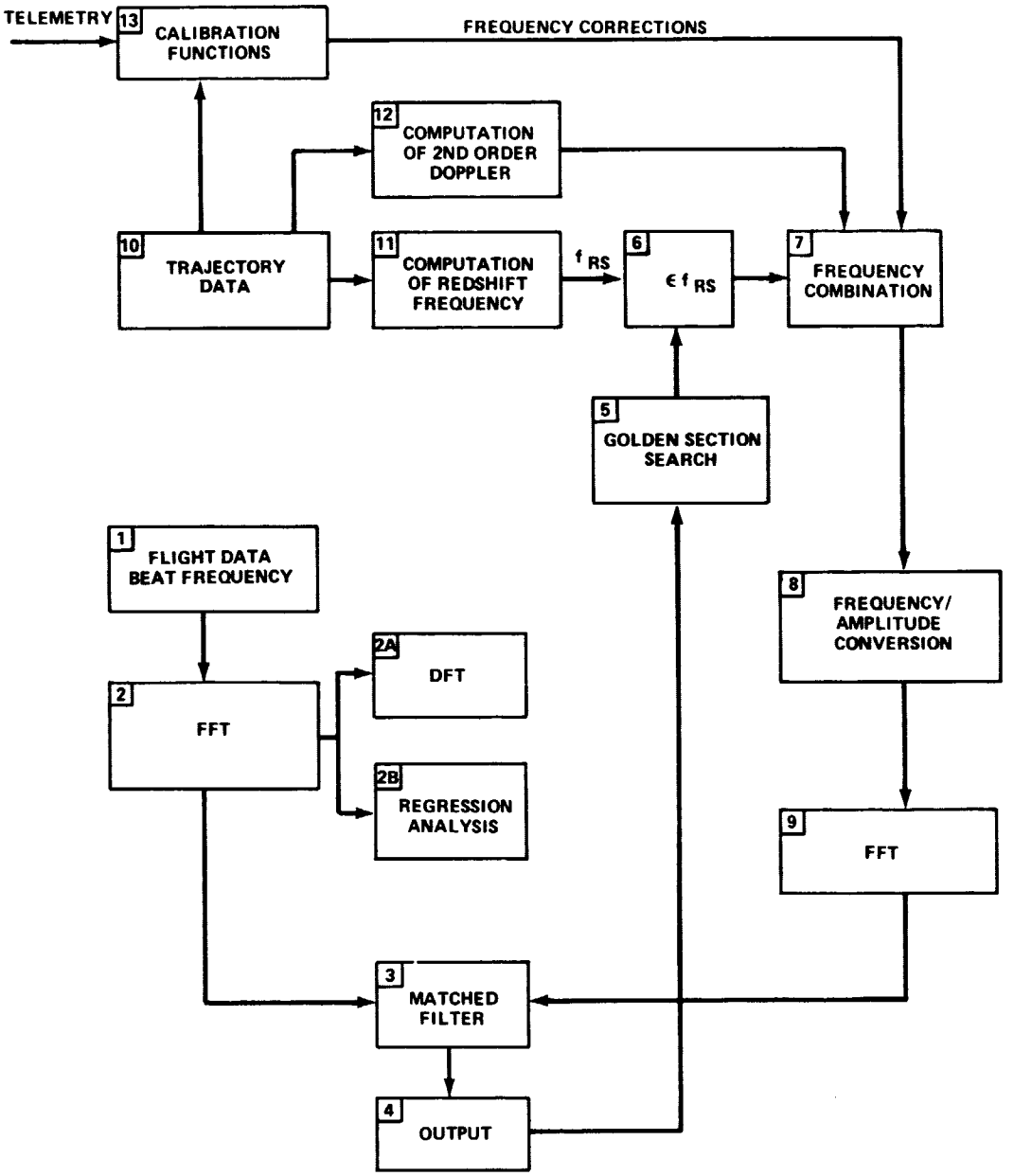

Figure 15. Data reduction flow chart.

REFERENCES

1. Vessot, Robert: Redshift Probe Experiment Critical Design Review, Smithsonian Astrophysical Observatory, Cambridge, Massachusetts, December 1974.

2. Vessot, Robert: Proceedings of the International School of Physics "Enrico Fermi" Experimental Gravitation, Academic Press, New York, 1974, pp. 111-162.

3. Bracewell, R. N.: The Fourier Transform and Its Applications, McGraw Hill, New York, 1965, pp. 160/163.

4. Brault, J. W. and White, O. R.: The Analysis and Restoration of Astronomical Data Via the Fast Fourier Transform. Astron. and Astrophys., vol. 13, 1971, pp. 169/189.

5. Cochran, W. T. and Cooley, W. T.: Special Issue on Fast Fourier Transform, IEEE Transactions on Audio and Electroacoustics, 1967, pp. 45/55.

6. Lanczos, C.: Discourse on Fourier Series. Hafner Publishing Co., New York, 1966, p. 139.

7. Singleton, R. C.: ALGOL Procedures for the Fast Fourier Transform. Collected Algorithms from CACM 338, p. 1.

8. Cook, C. E. and Bernfeld, M.: RADAR Signals. Academic Press, Inc., New York, 1967, Chapter 8.

9. Skolnik, M. J.: Introduction to RADAR Systems. McGraw Hill, New York, 1962, Chapter 9.

10. Cuccia, C. L.: Harmonics, Sidebands and Transients in Communication Engineering. McGraw Hill, New York, 1952, Chapter 15.

11. Rabiner, L. R. and Rader, C. M., (ed): Digital Signal Processing. IEEE Press, 1972, pp. 330/334.

12. Baugher, C. R.: The Effects of the GP-A Antenna on the Redshift Data, Space Sciences Laboratory internal memorandum, MSFC, December 1974 (available from author).

13. Bogner, R. E.: Statistical Stability in Spectrum Analysis. The Radio and Electronic Engineer, vol. 42, no. 9, September 1972.

APPROVAL

HIGH RESOLUTION FREQUENCY ANALYSIS TECHNIQUES WITH APPLICATION TO THE REDSHIFT EXPERIMENT

By R. Decher and D. Teuber

The information in this report has been reviewed for security classification. Review of any information concerning Department of Defense or Atomic Energy Commission programs has been made by the MSFC Security Classification Officer. This report, in its entirety, has been determined to be unclassified.

This document has also been reviewed and approved for technical accuracy.

Charles A. Lundquist

CHARLES A. LUNDQUIST
Director, Space Sciences Laboratory